Darcy Forchheimer flow of Williamson fluid past a stretching sheet with variable thermal conductivity

B. Das and S. Ahmed

Mathematics Department, Rajiv Gandhi University, Arunachal Pradesh, 791112, India
***Corresponding author**: bikash.das@rgu.ac.in; sahin.ahmed@rgu.ac.in

ABSTRACT The primary objective of this experiment is to examine the flow of a micropolar fluid through porous regime with microrotation in presence of magnetic field. The partial differential equations are first transformed into a coupled system of ODEs using appropriate similarity transformations. To solve the system of ODEs, BVP4C solver has been employed with relative tolerance of 10^{-6}. To make sure the present study is stable and convergent, all the outcomes are compared to the earlier findings. The impression of various parameters on velocity, temperature and microrotation profile are illustrated with the help of graph. The graph of entropy generation and skin friction and Nusselt number is also plotted against various governing parameters. Through this investigation it is found that Nusselt number can be increases by regulating the porous parameter and the viscosity of the Williamson fluid. The drag at the surface can be minimized by increasing the strength of magnetic field and Williamson fluid parameter. The implication of this study can be found in industrial field where entropy of the system plays an important role for better performance and stability.

KEYWORDS Entropy; Bejan number; Lorentz force; MHD

1. Introduction

Flow through stretching sheets has numerous applications in a range of scientific and technological domains, such as glass blowing, sheet manufacturing and metal coating etc. had gained interest of many researchers. First research on boundary layer along a constantly moving sheet was done by Sakiadis (1961). Numerical and analytical methods were adopted by Magyari and Keller (1999), to analyze the heat and mass diffusion by taking various physical configurations. The aforementioned discoveries motivated several researchers (Muskat, 1937; Collins, 1976) to investigate fluid flow behaviour in porous medium by employing Darcy's law to characterize convection. But in reality, the non-Darcy model is more trustworthy, where the fluid velocity is high. Tripathy et al. (2016) scrutinized the flow behaviour of micropolar fluid and the outcomes of heat source and chemical reaction over a stretching sheet with variable temperature using non-Darcy model. Pal and Mondal (2010) studied the influence of variable viscosity on mixed convective heat transmission across a porous material in presence of Lorentz force and by taking non-uniform heat generation/absorption into consideration using non-Darcy model. The numerical solution using HPM was obtained by Pattanaik et al. (2022) for the viscous fluid flow over a flat surface under the influence of Lorentz force. Pattnaik et al. (2022a) studied the flow behaviour of Fe_3O_4-water nanofluid over radially stretching sheet while considering the effects of the shape of nanoparticles. Some recent works on stretching are obtainable in refs. (Ratha et al., 2022; Shamshuddin et al., 2019a,b; Mishra and Bhatti, 2017; Tinker et al., 2022).

Since most fluids in real-world applications don't follow the standard Newtonian Navier-Stokes equations, modified equations are employed. Due to limitations of Newtonian fluids, the theory of micropolar fluid has received a lot of consideration in recent years from the engineering community. Micropolar fluids are the fluids which contain micro-structured gyrating particles, the presence of which can influence the hydrodynamics of the flow causing it to be markedly non-Newtonian. It may be used to study the behaviour of lubricants, the flow of liquid crystals, polymeric fluids and blood of human and animals (Khonsari, 1990; Busuke and Tatsuo, 1969; Lockwood et al., 1986; Lee and Eringen, 1971). Fluid microrotation was initially introduced by Eringen (1966). Kim and Lee (2003) investigated the problem of the micropolar fluid across a moving vertical porous plate of semi-infinite length in presence of magnetic field. The turbulent behaviour of a micropolar fluid's boundary layer flow was studied by Peddieson (1972). Salawu and Fatunmbi (2017) examined the micropolar fluid flow in presence of Lorentz force and variable electrical conductivity. Khan et al. (2014) studied hybrid ferromagnetic nanofluids by modelling microrotation and spin gradient viscosity. Farooq et al. (2017) investigated gyrotactic microorganisms in relation to sisco nanomaterial.

Williamson fluid was reported by Williamson (1929), is one of the most renowned non-Newtonian fluids. In order to analyze Williamson fluid flow with chemical reaction, Khan et al. (2014) adopted HAM. Numerous additional scholars, such as Nadeem et al. (2013), studied the pseudoplastic flow of Williamson fluid pasting stretched sheet analytically. Influence of magnetic field on Williamson nanofluid flow over a Darcy-Forchheimer porous medium was explored by Gautam et al. (2021) using numerical methods. Ahmed (2019) examined the influence of viscous dissipation, and thermal radiation on

DOI: 10.52292/j.laar.2024.3102
Received: February 5, 2023.
Accepted: July 15, 2023.
Recommended by Matteo D'Onorio.

heat transfer in Williamson fluid past a non-linear stretching sheet by using computational approach, Akbar et al. (2013) explored mathematically the peristaltic flow of Williamson nanofluid through an asymmetric conduit. Pattnaik et al. (2022b) studied the impact of radiation and viscous dissipation on the flow of a Williamson nanofluid within a parallel channel. Upreti et al. (2023a) investigated the influence of induced magnetic field on the motion of the Au-blood nanofluid by employing Cattaneo-Christov and Darcy Forchheimer model. In 2020, Upreti et al. (2020) studied the role of non-uniform heat source/sink on MHD flow of nanoinclusion of CNT in base fluid over a stretching surface under the influence of Lorentz force. Later, the authors (Upreti et al., 2023b,a) investigated the effects of various properties on the fluid motion of nanofluid in porous medium. A numerical study on unsteady flow of nanofluid over a stretching sheet embedded in porous medium was conducted by Gupta et al. (2023) and obtained the solutions for the effect of variable viscosity on the momentum and energy of the fluid.

In a thermodynamic system, the investigation of entropy generation is very significant due to its crucial role in engineering and industrial applications. The key concern of the researchers is to minimize the entropy generation to increase the efficiency and performance. In view of this, Bejan (1980) investigated entropy generation in a convective heat transfer process. Srinivasacharya and Hima Bindu (2016) investigated entropy generation due to flow of a micropolar fluid through a channel of parallel plates with constant pressure. Recently, Fatunmbi and Salawu (2020) studied the MHD flow of a micropolar fluid over a stretching impermeable plate saturated in non-Darcian media with non-homogeneous heat generation. A critical investigation on the entropy of the system due to the motion of hybrid nanofluid over a convective surface was carried out by Upreti et al. (2021).

The present investigation employs the Darcy Forchheimer model to study the motion of micropolar Williamson fluid over a non-linear stretching sheet under the action of Lorentz force. The novelty of the investigation is to study the effect of variable thermal conductivity over the entropy generated in the system. The effect of Forchheimer number on the fluid velocity and energy distribution was also taken into consideration in current investigation. To solve the non-linear governing partial differential equations, suitable similarity transformations has been adopted to convert the PDE's into system of ODE and then to obtain the solution of the differential equations MATLAB bvp4c program has been utilized and solutions are plotted for the effect of various parameters. The stability of the numerical method is also verified via grid point test and current study has also been validated with existing works.

2. Methods

2.1 Description of the problem

In this model, the flow of an incompressible Williamson micropolar fluid over a non-linear stretching surface with velocity $U_\infty x^r$ in a non-Darcian porous regime with space and temperature dependent heat source has been considered. Magnetic field of strength $B(x)$ is applied normal to the flow direction. $T_w = T_\infty + Ax^n$ is the temperature of the surface which is assumed to be variable and the temperature at free stream is assumed to be T_∞. Moreover, heating due to the presence of porous medium, viscous heating, ohmic heating and non-linear heat source has been considered in the energy equation. It is assumed that the magnetic Reynolds number is so small that the induced magnetic field can be neglected. Also, polarization of the charged particles is negligible, thus the hall current is also neglected.

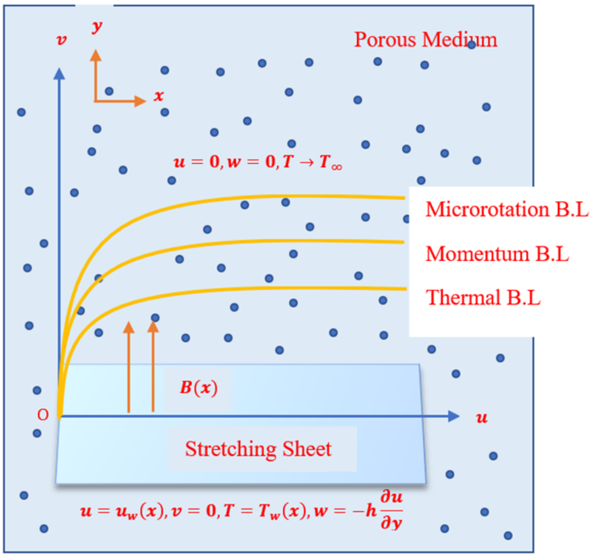

Figure 1: Schematic diagram of flow configuration.

The schematic diagram of the flow configuration is depicted in Fig. 1.

2.2 Mathematical formulation

With the help of contributions set by the investigators (Tripathy et al., 2016; Kumar, 2009; Fatunmbi and Salawu, 2020), the component-wise form of governing equations is:

$$\frac{\partial u}{\partial x} + \frac{\partial v}{\partial y} = 0 \tag{1}$$

$$u\frac{\partial w}{\partial x} + v\frac{\partial w}{\partial y} = \left\{ \begin{array}{l} \left(\frac{\mu + \mu_r}{\rho}\right)\frac{\partial^2 u}{\partial y^2} + \frac{\mu_r}{\rho}\frac{\partial w}{\partial y} + \\ \sqrt{2}\,\frac{\mu \Gamma}{\rho}\frac{\partial u}{\partial y}\frac{\partial^2 u}{\partial y^2} - \frac{\mu}{\rho k_p}u \\ -\frac{\sigma B(x)^2 u}{\rho} - \frac{Fs}{k_p}u^2 \end{array} \right\} \tag{2}$$

$$u\frac{\partial w}{\partial x} + v\frac{\partial w}{\partial y} = \frac{\gamma}{\rho_j}\frac{\partial^2 w}{\partial y^2} - \frac{\mu_r}{\rho_j}\left(2w + \frac{\partial u}{\partial y}\right) \tag{3}$$

$$u\frac{\partial T}{\partial x} + v\frac{\partial T}{\partial y} = \left\{ \begin{array}{l} \frac{1}{\rho C_p}\frac{\partial}{\partial y}\left(k^*\frac{\partial T}{\partial y}\right) + \left(\frac{\mu + \mu_r}{\rho C_p}\right) \\ \left(1 + \frac{\Gamma}{2}\frac{\partial u}{\partial y}\right)\left(\frac{\partial u}{\partial y}\right)^2 + \frac{\sigma B^2(x)}{\rho C_p}u^2 \\ + \frac{\mu}{\rho C_p k_p}u^2 + \frac{Fs}{C_p k_p}u^3 + \frac{q'''}{C_p} \end{array} \right\} \tag{4}$$

q''' is the non-uniform heat source following (Tripathy et al., 2016) and is given by:

$$q''' = \frac{U_w}{\nu x_r}\left[D^*(T-T_\infty)+c^*(T_w-T_\infty)\right] \tag{5}$$

where $C^* = \alpha x^{1-r}$ and $D^* = \beta x^{1-r}$ are the space and temperature dependent heat source with α and β being constants. $k^* = k_\infty(1+\varepsilon\theta)$ is the thermal conductivity and $\theta = \frac{T-T_w}{T_w-T_\infty}$.

The boundary conditions are as follows:

$$\left[\begin{array}{ll} y=0: & \left\{\begin{array}{l} u=u_w(x)=U_\infty x^r, \\ v=0,\ T=T(x)=T_\infty+Ax^n, \\ w=-h\dfrac{\partial u}{\partial y} \end{array}\right\} \\ y\to\infty: & \{u=0,\ w=0,\ T\to T_\infty\} \end{array}\right] \tag{6}$$

The condition of the boundary for microrotation has the following cases:

1. $h=0$, implies that $w=0$ and in such case, the micro-particles in the wall are fixed;
2. $h=1/2$, implies weak wall microrotation particles concentration;
3. $h=1$, can be applied for turbulent flow modelling.

Other boundary conditions have usual physical meaning.

Introducing the following similarity transformations (Rana and Bhargava, 2012):

$$\left\{\begin{array}{c} \eta = y\sqrt{\dfrac{U_\infty x^r(r+1)}{2\nu x}},\ u=U_\infty x^r f'(\eta), \\ v=-\sqrt{\dfrac{U_\infty \nu(r+1)}{2}}x^{\frac{r-1}{2}}\left[f+\left(\dfrac{r-1}{r+1}\right)\eta f'\right], \\ w=x^{\frac{3r-1}{2}}\left(\dfrac{U_\infty^3(r+1)}{2\nu}\right)^{\frac{1}{2}}g(\eta),\ \theta(\eta)=\dfrac{T-T_\infty}{T_w-T_\infty}, \\ \gamma=\left(\mu+\dfrac{\mu_r}{2}\right)j,\ j=\left(\dfrac{\nu}{U_\infty}\right)x^{1-r} \end{array}\right\} \tag{7}$$

On using (7), the system of equations 1-4 reduces to:

$$\left\{\begin{array}{l} (1+k)f'''+f\,f''+Wef'''f''+ \\ kg'-2\left(\dfrac{r+F_s}{r+1}\right)f^2-\dfrac{2}{r+1}(M+Da)f' \end{array}\right\}=0 \tag{8}$$

$$\left\{\begin{array}{l} (1+\varepsilon\theta)\theta''-2Pr\dfrac{n}{1+r}f'\theta+Prf\theta' \\ +(1+k)(1+Wef'')Brf''+ \\ \dfrac{2}{r+1}BrMf'^2\varepsilon\theta'^2+\left(\dfrac{2}{r+1}\right)BrDaf'^2 \\ +\left(\dfrac{2}{r+1}\right)BrFsf'^3+(\alpha f'+\beta\theta)\dfrac{2}{r+1} \end{array}\right\}=0 \tag{9}$$

$$\left\{\begin{array}{l} \left(1+\dfrac{k}{2}\right)g''+fg'-\dfrac{3r-1}{r+1}f'g \\ -k(2g+f'')\left(\dfrac{2}{r+1}\right) \end{array}\right\}=0 \tag{10}$$

with boundary conditions are as under:

$$\left[\begin{array}{ll} \eta=0: & \left\{\begin{array}{c} f'=1,\ f=0 \\ g=-hf'',\ \theta=1 \end{array}\right\} \\ \eta=6=\infty: & \{f'=0,\ g=0,\ \theta=0\} \end{array}\right] \tag{11}$$

Key quantities which include skin friction and local Nusselt number are given by:

$$\left\{C_f=\frac{\tau_w}{\rho U_w^2},\ Nu=\frac{xq_w}{k^*(T_w-T_\infty)}\right\}$$

where $\tau_w = \mu_r w + \frac{\Gamma}{2}\left(\frac{\partial u}{\partial y}\right)^2 + (\mu+\mu_r)\frac{\partial u}{\partial y}$ and $q_w = -k^*\left(\frac{\partial T}{\partial y}\right)_{y=0}$.

In non-dimensional form:

$$C_fRe^{\frac{1}{2}} = 2\left(\frac{r+1}{2}\right)^{\frac{1}{2}}\left[\begin{array}{c} \{1+k(1-h)\}f''(0) \\ +\dfrac{We}{2}f''(0)^2 \end{array}\right] \tag{12}$$

$$NuRe^{-\frac{1}{2}} = -\left(\frac{r+1}{2}\right)\theta'(0) \tag{13}$$

where

$$\left\{\begin{array}{c} M=\dfrac{2\sigma B_0^2x^{1-r}}{\rho_f U_\infty},\ Da=\dfrac{2\nu_f x^{1-r}}{k_pU_\infty},\ R=\dfrac{16\sigma_1T_\infty^3}{3\rho C_pk_1\nu}, \\ Ec=\dfrac{U_\infty^2}{C_p(T_w-T_\infty)},\ Pr=\dfrac{\nu_f}{\alpha_f},\ \nu_f=\dfrac{\mu_f}{\rho},\ k=\dfrac{\mu_r}{\mu}, \\ Fs=\dfrac{c_fx}{\sqrt{k_p^*}},\ We=\Gamma\sqrt{r+1}\sqrt{\dfrac{U_\infty^3}{\nu}}x^{\frac{3r-1}{2}}, \\ Re_x=\dfrac{U_\infty x}{\nu_f},\ Br=Pr\cdot Ec=\dfrac{\mu_f}{\rho\alpha_f}\dfrac{U_\infty^2}{C_p(T_w-T_\infty)} \end{array}\right\}$$

2.3 Formulation of entropy generation

According to the thermodynamic second law and irreversibility the formation of entropy generation:

$$S_{Gen}=\left\{\begin{array}{l} k^*\left(\dfrac{\nabla T}{T_\infty}\right)^2+\dfrac{(\mu+\mu_r)}{T_\infty}\left(\dfrac{du}{dy}\right)^2\left(1+\dfrac{\Gamma}{2}\dfrac{du}{dy}\right) \\ +\dfrac{\sigma B^2(x)}{T_\infty}u^2+\dfrac{\mu}{K_pT_\infty}u^2+\dfrac{Fs}{K_pT_\infty}u^3 \end{array}\right\}$$

The constituents in the entropy production are:

(a) Heat transmission,
(b) Viscous dissipation,
(c) Joule heating,
(d) Heating due to the presence of porous medium

Using the similarity transformation, the dimensionless form of entropy generation is given as:

$$\Delta=\frac{S_{Gen}}{S_0''},\ \text{where } S_0''=\frac{k^*\Omega^2U_\infty}{\nu}$$

Thus,

$$\Delta=\left\{\begin{array}{c} \theta'^2+\dfrac{Br}{\Omega(1+\varepsilon\theta)}(M+Da)f'^2+ \\ \dfrac{Br}{\Omega(1+\varepsilon\theta)}(1+K)(1+Wef'')f''^2 \\ +\dfrac{Br}{\Omega(1+\varepsilon\theta)}Fsf'^3 \end{array}\right\}$$

where

$$\Omega=\frac{T_w-T_\infty}{T_\infty}$$

3. Results and discussion

In this investigation, the behavior of Williamson micropolar fluid in non-Darcian porous medium with variable thermal conductivity is studied. To understand the behavior of motion in connection with the physical conditions, the graphs of velocity profile, micro-rotation profile and temperature profile and the numerical values of skin friction and Nusselt number are plotted. It is observed that the solutions are affected by Da, M, Fs, We and k which is explained below.

The variation of drag forces M and Da over the distributions of velocity, temperature and microrotation are plotted respectively in Figs. 2a – 2c. Fig. 2a designates the behaviour of the fluid velocity under the action of drag forces M and Da. The drag forces like magnetic field (M) and porosity (Da) always resists the motion of molecules of micropolar fluid and thereby decelerates the flow motion of molecules. The thickness of the momentum boundary layer has reduced by the impact of M and Da. Fig. 2b. illustrates the behaviour of the drag forces M and Da. The temperature of the micropolar fluid has raised under the action of M and Da and thereby the fluid becomes warm. The thickness of the thermal boundary layer has been inclined by virtue of the action of M and Da. Higher magnetic drag force generates higher temperature in the fluid region other than the lower Darcy drag force region.

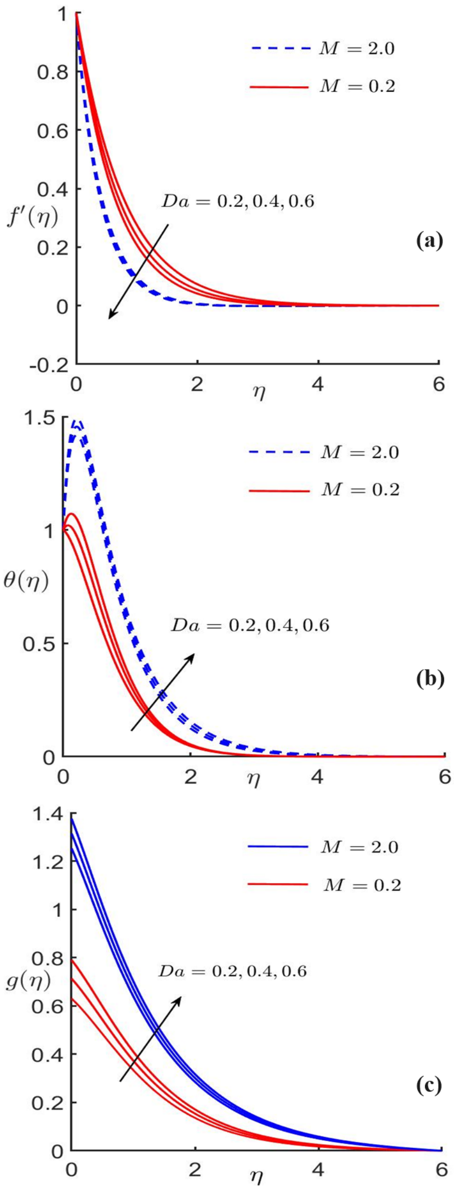

Figure 2: Variation of M and Da over a) the velocity; b) the temperature; c) the microrotation.

The dual solution of $g(\eta)$ for the magnetic drag force for $M = 0.2$ and $M = 2.0$ with the variation of porosity drag (Da) have been plotted in Fig. 2c. As micropolar fluid, due to rotation creates a vortex tube and therefore, the impact of rotation is higher than the drag forces like magnetic field and Darcy's porosity. Hence, the molecules of the micropolar fluid over the microrotation profiles are moving forward and inclines the microrotation curves under the action of M and Da. Higher magnetic drag force generates the higher values of $g(\eta)$.

The impact of We and Fs over the velocity, microrotation and temperature profile are illustrated in Fig. 3a – 3c. It is observed that the fluid velocity decreases as the inertial coefficient or Forcheimmer number Fs increases. This is due to the fact that the inertial coefficient provides additional resistance to the fluid which decreases the fluid velocity which in turn rises the temperature. Thus, the Forcheimmer drag depresses the fluid velocity but has a positive impact on the temperature. The Weissenberg number is a dimensionless parameter used to describe the viscoelastic behavior of a fluid flow. It characterizes the relative importance of elastic effects compared to viscous effects. When the Weissenberg number increases, it indicates a stronger influence of elastic properties and the elastic effects become more dominant, leading to the deformation and stretching of the fluid. These elastic effects resist the flow and can slow down the fluid velocity.

When rotation parameter increases, the kinematic viscosity decreases as a result fluid velocity increases which can be observed in Fig. 4a. When considering fluid flow over a stretching sheet, the decrease in fluid velocity with increasing Forchheimer number suggests that inertial effects become less significant, and the flow is primarily governed by viscous forces. As a result, the flow tends to become more uniform and less influenced by fluid inertia. In the case of a Williamson fluid flowing over a stretching sheet, an increase in the microrotation parameter would suggest a greater degree of rotational effects within the fluid flow. This can lead to an increase in the fluid velocity.

The effect of thermal conductivity over the entropy is illustrated in Fig. 5a. Entropy generation has a tendency to diminish the rate of change of temperature in the porous media due to the impact of augmentation of thermal conductivity. In physical point of view, increase in thermal conductivity, the temperature dissipation rises that causes the lower kinetic energy of molecules of the fluid and, as a result, entropy generation reduces. Entropy generation refers to the production of entropy within a system. In the

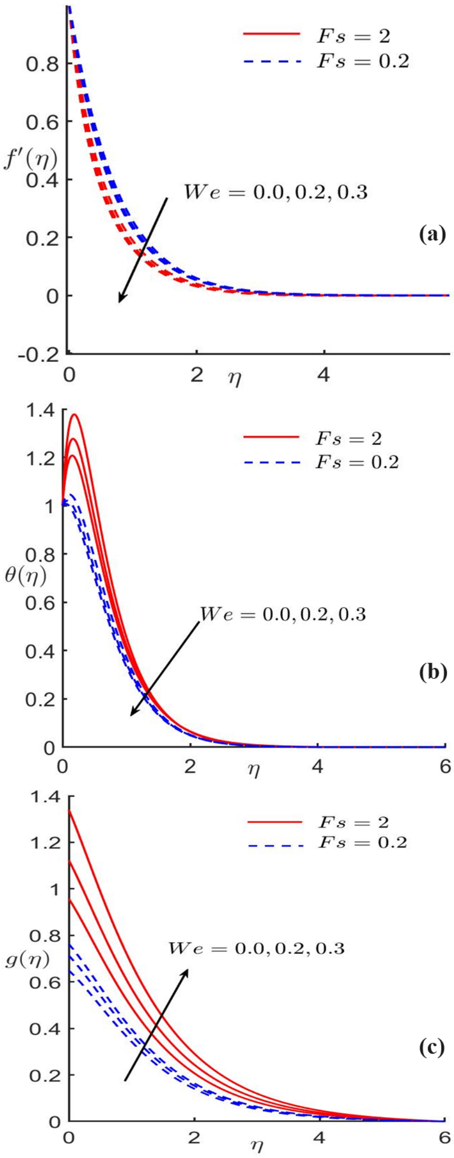

Figure 3: Variation of We and Fs over a) the velocity; b) the temperature; c) the microrotation.

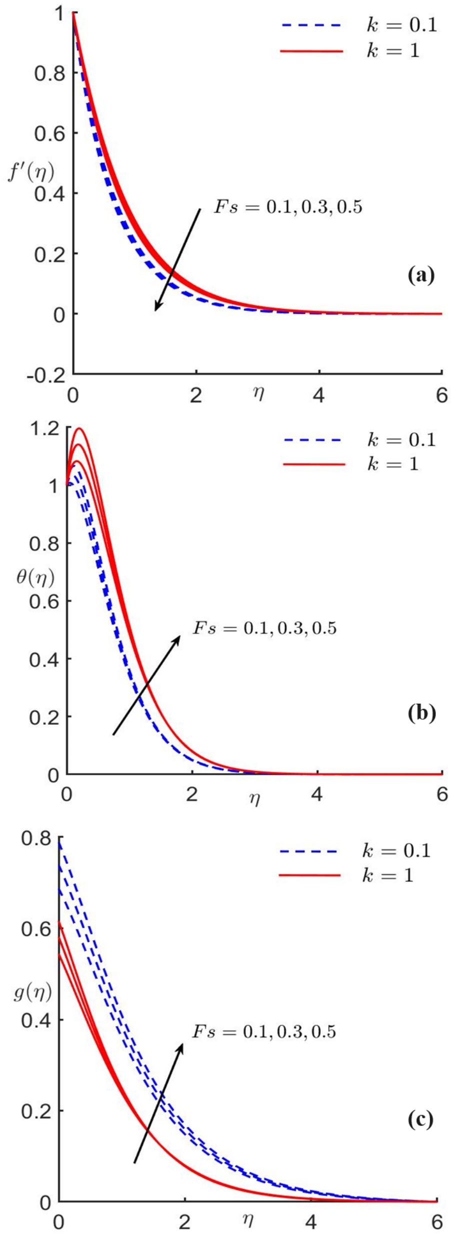

Figure 4: Variation of k and Fs over a) the velocity; b) the temperature; c) the microrotation.

context of fluid flow, it is associated with the irreversibilities and dissipative processes occurring in the flow field. These irreversibilities contribute to the generation of heat and the overall decrease in system efficiency.

Influence of k, We and M over skin friction is illustrated in Fig. 6. With rising microrotation, the skin friction increases significantly. Whereas, Lorentz force reduces the skin friction. This is due to the fact that, the Lorentz force retards the fluid motion which ultimately reduces the frictional force at the surface. Hence, decline in the skin friction has been reported in Fig. 6. Fig. 7a – 7b, depicts the impact of We, Br, Fs and M over Nusselt number. The rate of heat transfer at the surface declines with augmented values of M, Br, Fs, Da and We.

The non-linear system of ODEs given by 8 to 12 are solved numerically using BVP4C solver in MATLAB with $\Delta\eta = 0.001$. The converged results are within the tolerance limit of 10^{-6}. The result obtained satisfies the boundary conditions asymptotically. Which indicates the accuracy of the results. BVP4C is a MATLAB program that uses the finite difference code which implements the three stage Lobatto illa formula. This method provides a solution of fourth order which is accurate and uniform in the range of integration. Fig. 8 demonstrates the flow chart of the bvp4c solver.

Let,

$$\left\{\begin{array}{c} f = y(1),\ f'(2),\ f'' = y(3) \\ \theta = y(4),\ \theta' = y(5) \\ g = y(6),\ g' = y(7) \end{array}\right\}$$

From the system of O.D.E 8 to 10 with the above

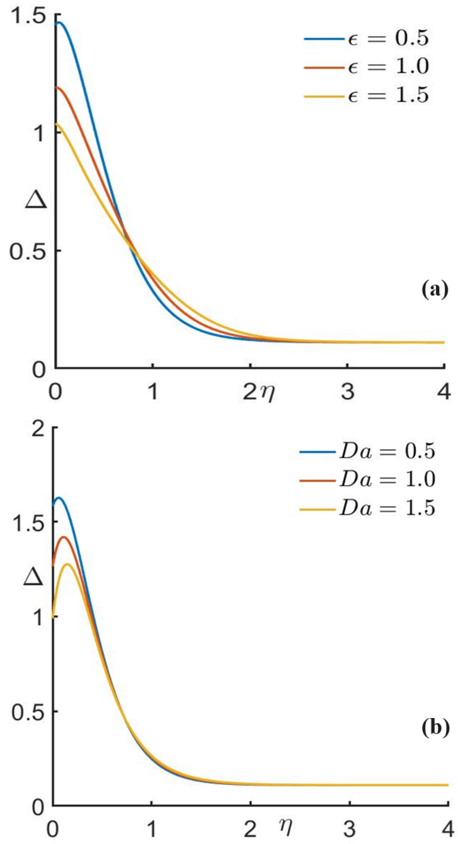

Figure 5: a) Impact of variable thermal conductivity over entropy generation. b) Variation of *Da* over entropy generation

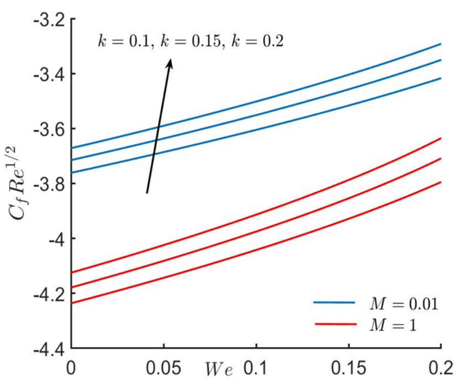

Figure 6: Impact of *Da*, *k*, *We* and *M* over skin friction.

considerations, we get

$$y'(3) = \left\{ \left(\frac{1}{1+k+We\, y(3)} \right) \left[\begin{array}{c} -y(1)y(3) \\ -ky(7)+2y(2)^2+ \\ \left(\frac{2}{r+1}\right)(M+Da)\,y(2) \end{array} \right] \right\} \tag{14}$$

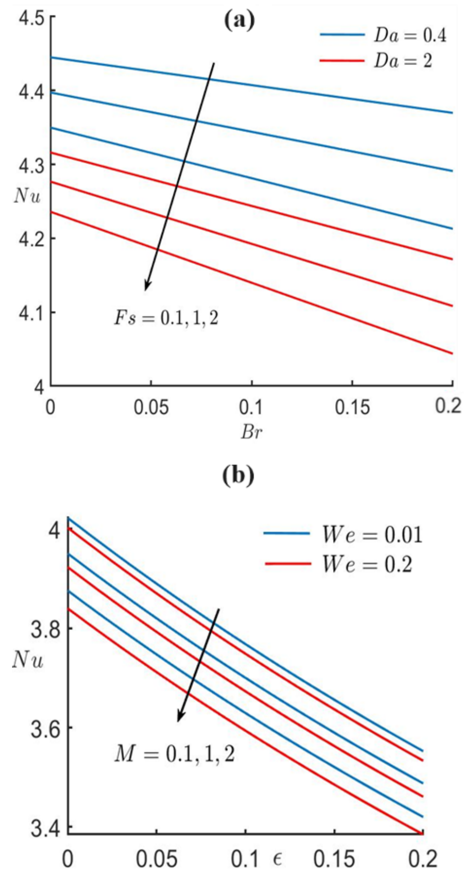

Figure 7: (a) - (b): Impact of *We*, *Br*, *Fs* and *M* over Nusselt number.

$$y'(5) = \left\{ \begin{array}{l} \left(\frac{1}{1+\varepsilon y(4)}\right)\left(\frac{2Pr\, n}{1+r}\right) y(2)y(4) \\ -Pr\, y(1)y(5)-(1-k) \\ (1+We\, y(3))\, Br\, y(3)^2 \\ -\left(\frac{2}{r+1}\right) BrMy(2)^2 - \\ \varepsilon y(5)^2 - \left(\frac{2}{r+1}\right) BrDa\, y(2)^2 \\ -\left(\frac{2}{r+1}\right) BrFs\, y(2)^3 - \\ (\alpha y(2)+\beta y(4))\left(\frac{2}{r+1}\right) \end{array} \right\} \tag{15}$$

$$y'(7) = \left\{ \left(\frac{1}{1+\frac{k}{2}}\right) \left[\begin{array}{c} -y(1)y(7)+ \\ \left(\frac{3r-1}{r+1}\right) y(2)y(6)+ \\ k(2y(6)+y(3))\left(\frac{2}{r+1}\right) \end{array} \right] \right\} \tag{16}$$

subject to boundary conditions:

$$\left[\begin{array}{ll} \eta = 0: & \left\{ \begin{array}{c} y(2)=1,\ y(1)=0, \\ y(6)=-hy(3), \\ y(4)=1 \end{array} \right\} \\ \eta = 6 = \infty: & \left\{ \begin{array}{c} y(2)=y(4)=0 \\ y(6)=0 \end{array} \right\} \end{array} \right] \tag{17}$$

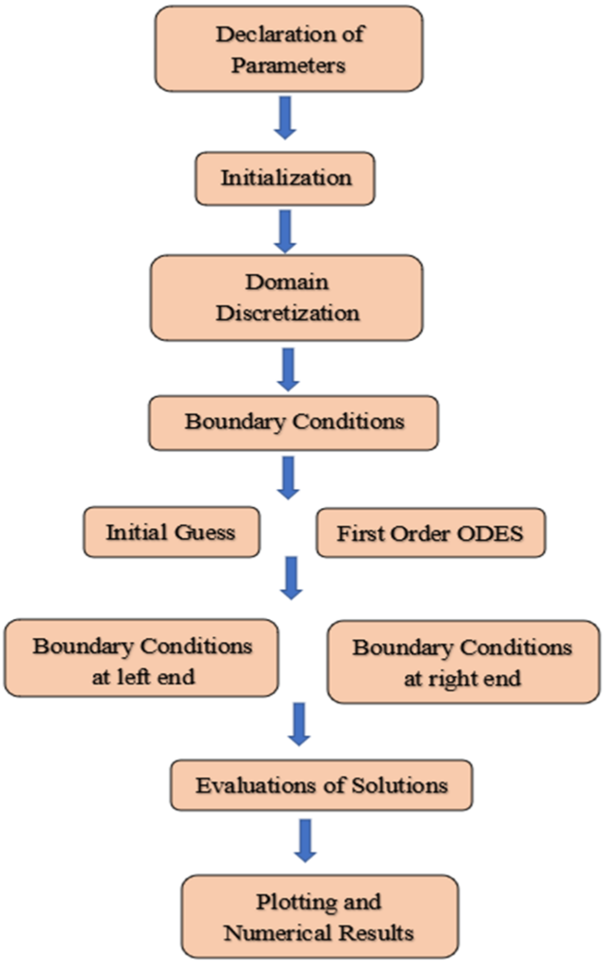

Figure 8: Flow chart of BVP4C solver.

4. Conclusions

Following previous research, the problem is formulated in two-dimensional component-wise form with appropriate boundary conditions, then translated to ODEs via similarity transformations. The BVP4C Solver is employed to solve these ODEs numerically. Finally, numerous graphs show the influence of the regulating factors. Finally impact of the governing parameters, are illustrated by several graphs. Influence of pertinent parameter on skin friction has been computed and illustrated in Table 1. Present work has been compared with the existing work and presented in Table 1 and Table 2. From both the tables it is evident the behavior of both skin friction and Nusselt number for various parameters are similar with the existing data. The stability of the adopted scheme is presented in Table 3. It is evident that the difference of any physical variables for $\eta = 0.001$ and $\eta = 0.0001$ is negligible. Therefore, the adopted scheme is stable and convergent.

Effort in this study addressed the theoretical and computational analysis of Forchheimer flow of Williamson fluid in the presence of Lorentz force past a stretching sheet. In addition to this, analysis on the entropy generation has been made. The following conclusions has been drawn through the investigation:

1. Velocity of the fluid can be regulated by varying M, Da, We, Fs and k. Decline in fluid velocity is observed with the augmented values of M, Da, We, Fs. Whereas, k enhances fluid velocity.
2. Rise in the fluid temperature is reported with the rising values of M, Da, Fs and k. Whereas, We decreases the temperature of the fluid.
3. Escalating values of M, Da, Fs, k, We intensifies the microrotation.
4. Coefficient of skin friction is an increasing function of We and k. But Lorentz force reduces the skin friction.
5. The rate of heat transfer at the surface can be increased by increasing Da and We.

Table 1: Variation in skin friction $-f''(0)$ when $Pr = 0.001$, $Br = 0.02$, $\alpha = 0.1$, $\beta = 0.1$, $n = 1$, $h = 0.5$.

k	Da	F	Kumar (2009)	Mishra et al. (2022)	Present
0.5	1	1	2.0191	1.8509	2.0055
0.7	1	1	1.9604	1.8046	1.9396
1	1	1	1.8885	1.7477	1.8613
0.5	1.5	1	2.1777	2.0191	2.1891
0.5	2.0	1	2.3279	2.1777	2.3640
0.5	2.5	1	2.4708	2.3279	2.5313
0.5	1	1.5	2.1292	1.9687	2.1331
0.5	1	2.0	2.2344	2.0806	2.2553
0.5	1	2.5	2.3352	2.1874	2.3728

Table 2: Variation in Nusselt number $\theta'(0)$ when $Ec = 1$, $\alpha = 0.1$, $\beta = 0.1$, $n = 1$, $h = 0.5$, $Fs = 2.5$, $We = 0.1$, $r = 0.01$, $M = 0.2$, $\varepsilon = 0.1$.

k	Da	Br	Kumar (2009)	Mishra et al. (2022)	Present
0.5	1	1	0.3582	0.3923	0.6495
0.7	1	1	0.4910	0.5131	0.7705
1	1	1	0.6875	0.6910	0.9530
0.5	1.5	1	0.6324	0.6325	0.8565
0.5	2.0	1	0.8890	0.8537	0.9795
0.5	2.5	1	1.1302	1.0583	1.1335
0.5	1	1.5	1.0341	1.0814	1.3497
0.5	1	2.0	1.7070	1.7696	2.0330
0.5	1	2.5	2.3763	2.4568	2.6954

Table 3: Grid point stability test.

$\Delta\eta = 0.001$				$\Delta\eta = 0.0001$			
η	f'	θ	g	η	f'	θ	g
0	1.0000	1.0000	0.6702	0	1.0000	1.0000	0.6702
1	0.2762	0.1063	0.3519	1	0.2762	0.1063	0.3519
2	0.0782	0.0081	0.1434	2	0.0782	0.0081	0.1434
3	0.0216	0.0016	0.0533	3	0.0216	0.0016	0.0533
4	0.0056	0.0008	0.0185	4	0.0056	0.0008	0.0185
5	0.0012	0.0005	0.0053	5	0.0012	0.0005	0.0053
6	0	0	0	6	0	0	0

Nomenclature

Br: Brinkmann number
C^*: Space dependent heat source
C_p: Specific heat
D^*: Temperature dependent heat source
Da: Porous parameter
Ec: Eckert number

Fs: Inertia coefficient
g: Microrotation profile
h: Microrotation boundary parameter
K: Material parameter
k^*: Thermal conductivity
k: Microrotation parameter
M: Magnetic parameter
n: Surface temperature parameter
Pr: Generalize Prandtl number
q''': Generalize Prandtl number
T: Temperature inside the boundary layer
T_w: Fluid temperature at wall
T_∞: Free stream temperature
U_∞: Stretching velocity parameter
(u,v): Velocity component along x,y direction
V_∞: Reference kinematic viscosity
We: Williamson parameter/Weissenberg number
(x,y): Cartesian coordinates
ε: Variable coefficient of thermal conductivity
Γ: Williamson kinematic viscosity
η: Similarity variable
θ: Dimensionless temperature
ν: Kinematic viscosity
μ: Dynamic viscosity
μ_r: vortex viscosity
σ: Electrical conductivity

References

Ahmed, M. M. (2019). Williamson fluid flow due to a nonlinearly stretching sheet with viscous dissipation and thermal radiation. *Journal of the Egyptian Mathematical Society*, 27:1–10.

Akbar, N. S., Nadeem, S., Lee, C., Khan, Z. H., and Haq, R. U. (2013). Numerical study of Williamson nano fluid flow in an asymmetric channel. *Results in Physics*, 3:161–166.

Bejan, A. (1980). Second law analysis in heat transfer. *Energy*, 5(8-9):720–732.

Busuke, H. and Tatsuo, T. (1969). Two-dimensional shear flows of linear micropolar fluids. *International Journal of Engineering Science*, 7(5):515–522.

Collins, R. (1976). *Flow of Fluids through Porous Materials*. PennWell Publishing Company, Tulsa, Oklahoma, USA.

Eringen, A. (1966). Theory of micropolar fluids. *Journal of Mathematics and Mechanics*, pages 1–18.

Farooq, S., Hayat, T., Alsaedi, A., and Ahmad, B. (2017). Numerically framing the features of second order velocity slip in mixed convective flow of Sisko nanomaterial considering gyrotactic microorganisms. *International Journal of Heat and Mass Transfer*, 112:521–532.

Fatunmbi, E. and Salawu, S. (2020). Thermodynamic second law analysis of magneto-micropolar fluid flow past nonlinear porous media with non-uniform heat source. *Propulsion and Power Research*, 9(3):281–288.

Gautam, A. K., Verma, A. K., Bhattacharyya, K., Mukhopadhyay, S., and Chamkha, A. J. (2021). Impacts of activation energy and binary chemical reaction on MHD flow of Williamson nanofluid in Darcy-Forchheimer porous medium: a case of expanding sheet of variable thickness. *Waves in Random and Complex Media*, pages 1–22.

Gupta, T., Pandey, A. K., and Kumar, M. (2023). Numerical study for temperature-dependent viscosity based unsteady flow of GP-MoS_2/$C_2H_6O_2$-H_2O over a porous stretching sheet. *Numerical Heat Transfer, Part A: Applications*, pages 1–22.

Khan, N. A., Khan, S., and Riaz, F. (2014). Boundary layer flow of Williamson fluid with chemically reactive species using scaling transformation and homotopy analysis method. *Mathematical Sciences Letters*, 3(3):199–205.

Khonsari, M. M. (1990). On the self-excited whirl orbits of a journal in a sleeve bearing lubricated with micropolar fluids. *Acta Mechanica*, 81(3-4):235–244.

Kim, Y. J. and Lee, J.-C. (2003). Analytical studies on MHD oscillatory flow of a micropolar fluid over a vertical porous plate. *Surface and Coatings Technology*, 171(1-3):187–193.

Kumar, L. (2009). Finite element analysis of combined heat and mass transfer in hydromagnetic micropolar flow along a stretching sheet. *Computational Materials Science*, 46(4):841–848.

Lee, J. D. and Eringen, A. C. (1971). Boundary effects of orientation of nematic liquid crystals. *The Journal of Chemical Physics*, 55(9):4509–4512.

Lockwood, F. E., Benchaita, M. T., and Friberg, S. E. (1986). Study of lyotropic liquid crystals in viscometric flow and elastohydrodynamic contact. *A S L E Transactions*, 30(4):539–548.

Magyari, E. and Keller, B. (1999). Heat and mass transfer in the boundary layers on an exponentially stretching continuous surface. *Journal of Physics D: Applied Physics*, 32(5):577–585.

Mishra, P., Kumar, D., Kumar, J., Abdel-Aty, A.-H., Park, C., and Yahia, I. S. (2022). Analysis of MHD Williamson micropolar fluid flow in non-Darcian porous media with variable thermal conductivity. *Case Studies in Thermal Engineering*, 36:102195.

Mishra, S. and Bhatti, M. (2017). Simultaneous effects of chemical reaction and Ohmic heating with heat and mass transfer over a stretching surface: A numerical study. *Chinese Journal of Chemical Engineering*, 25(9):1137–1142.

Muskat, M. (1937). *The Flow of Homogeneous Fluids through Porous Media: Analogies with other Physical Problems*. McGraw-Hill.

Nadeem, S., Hussain, S. T., and Lee, C. (2013). Flow of a Williamson fluid over a stretching sheet. *Brazilian Journal of Chemical Engineering*, 30(3):619–625.

Pal, D. and Mondal, H. (2010). Effect of variable viscosity on MHD non-Darcy mixed convective heat transfer over a stretching sheet embedded in a porous medium with non-uniform heat source/sink. *Communications in Nonlinear Science and Numerical Simulation*, 15(6):1553–1564.

Pattanaik, P. C., Mishra, S., Jena, S., and Pattnaik, P. (2022). Impact of radiative and dissipative heat on the Williamson nanofluid flow within a parallel channel due to thermal buoyancy. *Proceedings of the Institution of Mechanical Engineers, Part N: Journal of Nanomaterials, Nanoengineering and Nanosystems*, 236(1-2):3–18.

Pattnaik, P. K., Pattnaik, J. R., and Mishra, S. R. (2022a). Illustration of low-pressure gradient on the MHD flow of viscous fluid over a flat plate: the Homotopy Perturbation Method. *Waves in Random and Complex Media*, pages 1–19.

Pattnaik, P. K., Pattnaik, J. R., Mishra, S. R., and Nisar, K. S. (2022b). Variation of the shape of Fe3O4-nanoparticles on the heat transfer phenomenon with the inclusion of thermal radiation. *Journal of Thermal Analysis and Calorimetry*, 147(3):2537–2548.

Peddieson, J. (1972). An application of the micropolar fluid model to the calculation of a turbulent shear flow. *International Journal of Engineering Science*, 10(1):23–32.

Rana, P. and Bhargava, R. (2012). Flow and heat transfer of a nanofluid over a nonlinearly stretching sheet: A numerical study. *Communications in Nonlinear Science and Numerical Simulation*, 17(1):212–226.

Ratha, P. K., Mishra, S., Tripathy, R., and Pattnaik, P. K. (2022). Analytical approach on the free convection of Buongiorno model nanofluid over a shrinking surface. *Proceedings of the Institution of Mechanical Engineers, Part N: Journal of Nanomaterials, Nanoengineering and Nanosystems*.

Sakiadis, B. C. (1961). Boundary-layer behavior on continuous solid surfaces: I. Boundary-layer equations for two-dimensional and axisymmetric flow. *AIChE Journal*, 7(1):26–28.

Salawu, S. and Fatunmbi, E. (2017). Dissipative heat transfer of micropolar hydromagnetic variable electric conductivity fluid past inclined plate with joule heating and non-uniform heat generation. *Asian Journal of Physical and Chemical Sciences*, 2(1):1–10.

Shamshuddin, M., Mishra, S. R., Bég, O. A., and Kadir, A. (2019a). Numerical study of heat transfer and viscous flow in a dual rotating extendable disk system with a non-Fourier heat flux model. *Heat Transfer—Asian Research*, 48(1):435–459.

Shamshuddin, M., Mishra, S. R., Bég, O. A., and Kadir, A. (2019b). Viscous dissipation and Joule heating effects in non-Fourier MHD squeezing flow, heat and mass transfer between riga plates with thermal radiation: Variational parameter method solutions. *Arabian Journal for Science and Engineering*, 44(9):8053–8066.

Srinivasacharya, D. and Hima Bindu, K. (2016). Entropy generation in a micropolar fluid flow through an inclined channel. *Alexandria Engineering Journal*, 55(2):973–982.

Tinker, S., Mishra, S., Pattnaik, P., and Sharma, R. P. (2022). Simulation of time-dependent radiative heat motion over a stretching/shrinking sheet of hybrid Nanofluid: Stability analysis for dual solutions. *Proceedings of the Institution of Mechanical Engineers, Part N: Journal of Nanomaterials, Nanoengineering and Nanosystems*, 236(1-2):19–30.

Tripathy, R., Dash, G., Mishra, S., and Hoque, M. M. (2016). Numerical analysis of hydromagnetic micropolar fluid along a stretching sheet embedded in porous medium with non-uniform heat source and chemical reaction. *Engineering Science and Technology, an International Journal*, 19(3):1573–1581.

Upreti, H., Bartwal, P., Pandey, A. K., and Makinde, O. D. (2023a). Heat transfer assessment for Au-blood nanofluid flow in Darcy-Forchheimer porous medium using induced magnetic field and Cattaneo-Christov model. *Numerical Heat Transfer, Part B: Fundamentals*, 84(4):415–431.

Upreti, H., Pandey, A. K., and Kumar, M. (2021). Assessment of entropy generation and heat transfer in three-dimensional hybrid nanofluids flow due to convective surface and base fluids. *Journal of Porous Media*, 24(3):35–50.

Upreti, H., Pandey, A. K., Kumar, M., and Makinde, O. D. (2020). Ohmic heating and non-uniform heat source/sink roles on 3D Darcy-Forchheimer flow of CNTs nanofluids over a stretching surface. *Arabian Journal for Science and Engineering*, 45(9):7705–7717.

Upreti, H., Pandey, A. K., Kumar, M., and Makinde, O. D. (2023b). Darcy-Forchheimer flow of CNTs-H_2O nanofluid over a porous stretchable surface with Xue model. *International Journal of Modern Physics B*, 37(02).

Williamson, R. V. (1929). The flow of pseudoplastic materials. *Industrial & Engineering Chemistry*, 21(11):1108–1111.